

# Analyses of Phase Scintillation Observations Made by a Static Triple Frequency GPS-based Monitor Located Near the Equatorial Ionization Anomaly Peak

E.R. DE PAULA<sup>1</sup>, A.O. MORAES<sup>2</sup>, E. COSTA<sup>3</sup>, F. RODRIGUES<sup>4</sup>, M.A. ABDU<sup>1,5</sup>, K. OLIVEIRA<sup>6</sup> AND W.J. PERRELLA<sup>5</sup>

1) INPE São José dos Campos, SP, Brazil email:eurico@dae.inpe.br, 2) IAE, São José dos Campos, SP, Brazil, 3) CETUC/PUC-Rio de Janeiro, RJ, Brazil, 4) UTD, Dallas, TX, USA, 5) ITA, São José dos Campos, SP, Brazil 6) IFECT Goiania, GO, Brazil

## 1) Introduction:

Ionospheric scintillation is a manifestation of space weather effects that seriously affect the performance and availability of space-based navigation and communication systems. This paper presents results from an investigation on the characteristics of the phase and amplitude scintillation of Global Positioning System signals at the L1, L2C and L5 frequencies. Field data obtained by a scintillation monitor installed in São José dos Campos (23.1°S; 45.8°W; dip latitude 17.3°S, declination 21.4° W), Brazil, a station located near the southern crest of the Equatorial Ionization Anomaly, was used for this purpose. The analyzed data was collected during 150 nights from November 2014 to March 2015, an epoch of moderate solar activity close to the recent solar maximum. Only measurements corresponding to an elevation mask of 30° and values above standard threshold levels were used in the analysis. The study emphasizes phase scintillation ( $\sigma_\phi$ ), but also involves comparisons with amplitude scintillation (S4). The different characteristics of scintillation focused in this study include: (1) the day-to-day variation in the diurnal average and maximum intensity; (2) the local time distribution of phase scintillation at different intensity levels; (3); azimuth-elevation (spatial) distributions at different level of the standard deviation of phase fluctuations; (4) the relationship between amplitude and phase scintillation parameters for the L1, L2C, and L5 carriers of the Global Positioning System; and (5) the frequency dependence of the amplitude and phase scintillation parameters. Important results on these different characteristics are presented. A brief summary of the main results and some conclusions are presented below. Figure 1 shows TEC, S4 and  $\sigma_\phi$  for PRN 25 on November 13, 2014 for L1, L2C, and L5 carriers.

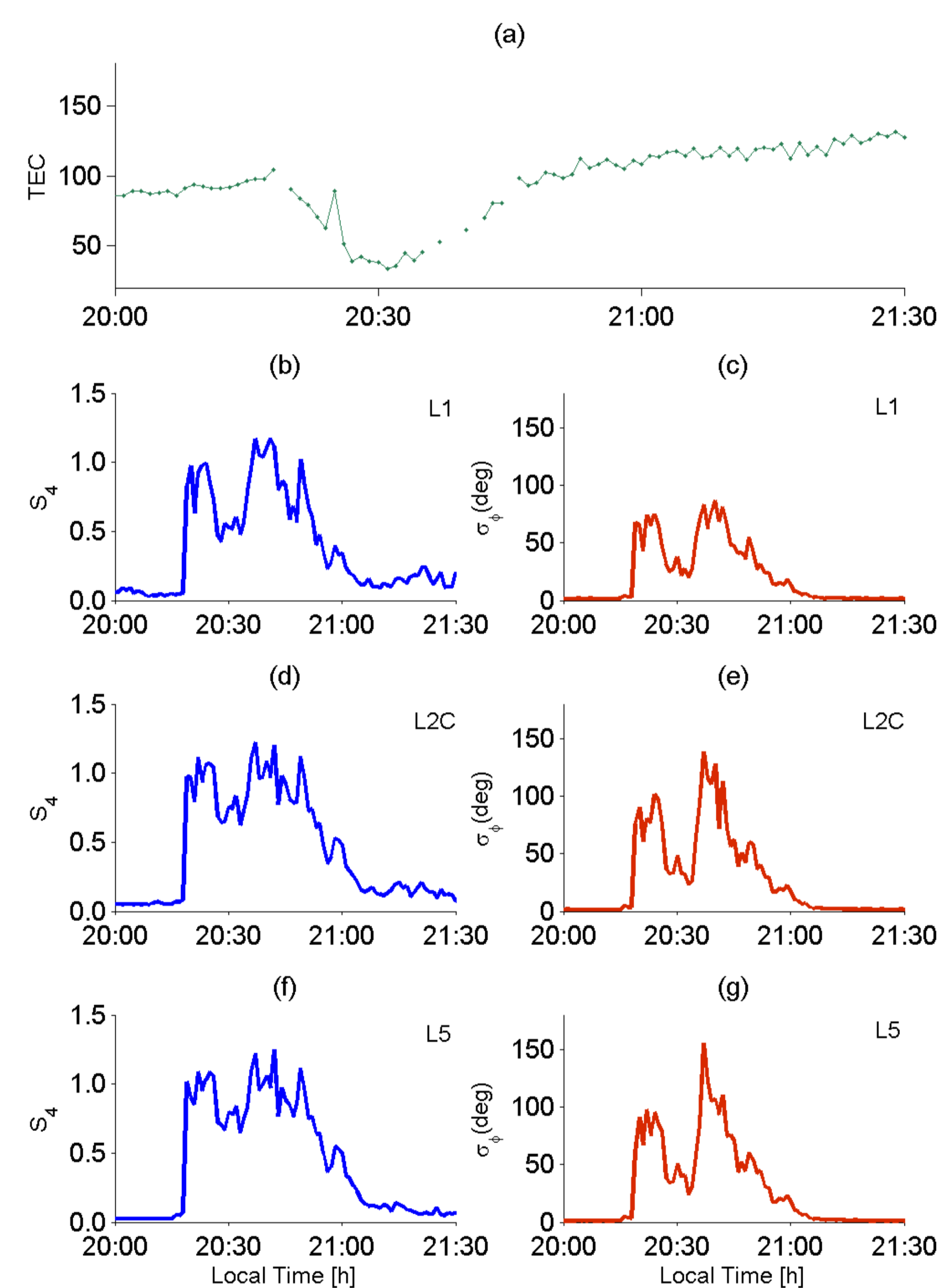


**Figure 1** – Panel (a) shows the relative TEC for PRN 25 on November 13 2014 in TEC units ( $10^{16}$  el/m<sup>2</sup>); Panels (b), (d) and (f) display the corresponding S4 indices for the L1, L2C and L5 signals, respectively; Panels (c), (e) and (g) display the corresponding  $\sigma_\phi$  indices for the L1, L2C and L5 signals, respectively.

## 2) Phase Scintillation ( $\sigma_\phi$ ) Daily Variation:

The daily average values of  $\sigma_\phi$  varied from approximately 10° to 60°, the corresponding maximum values reached 270°. Their day-to-day variation patterns presented smaller values during the month of January (Figure 2), with fluctuations at larger intensity observed in other months. The overall result showed that the daily average values of  $\sigma_\phi$  L2C and  $\sigma_\phi$  L5 exceeded the corresponding values of  $\sigma_\phi$  L1 in 55 % and 65 % of the cases, respectively. The daily maximum values also showed a similar tendency. Furthermore, the results also showed that, considering only the satellites that transmit the three signals, phase scintillation events with  $\sigma_\phi > 8.6^\circ$  at the L5 frequency lasted longer than those at the L1 and L2C frequencies in 87.39 % and 58.82 % of cases, respectively. These results clearly indicate that the new lower L-band GPS frequencies are more susceptible to scintillation than the higher one.

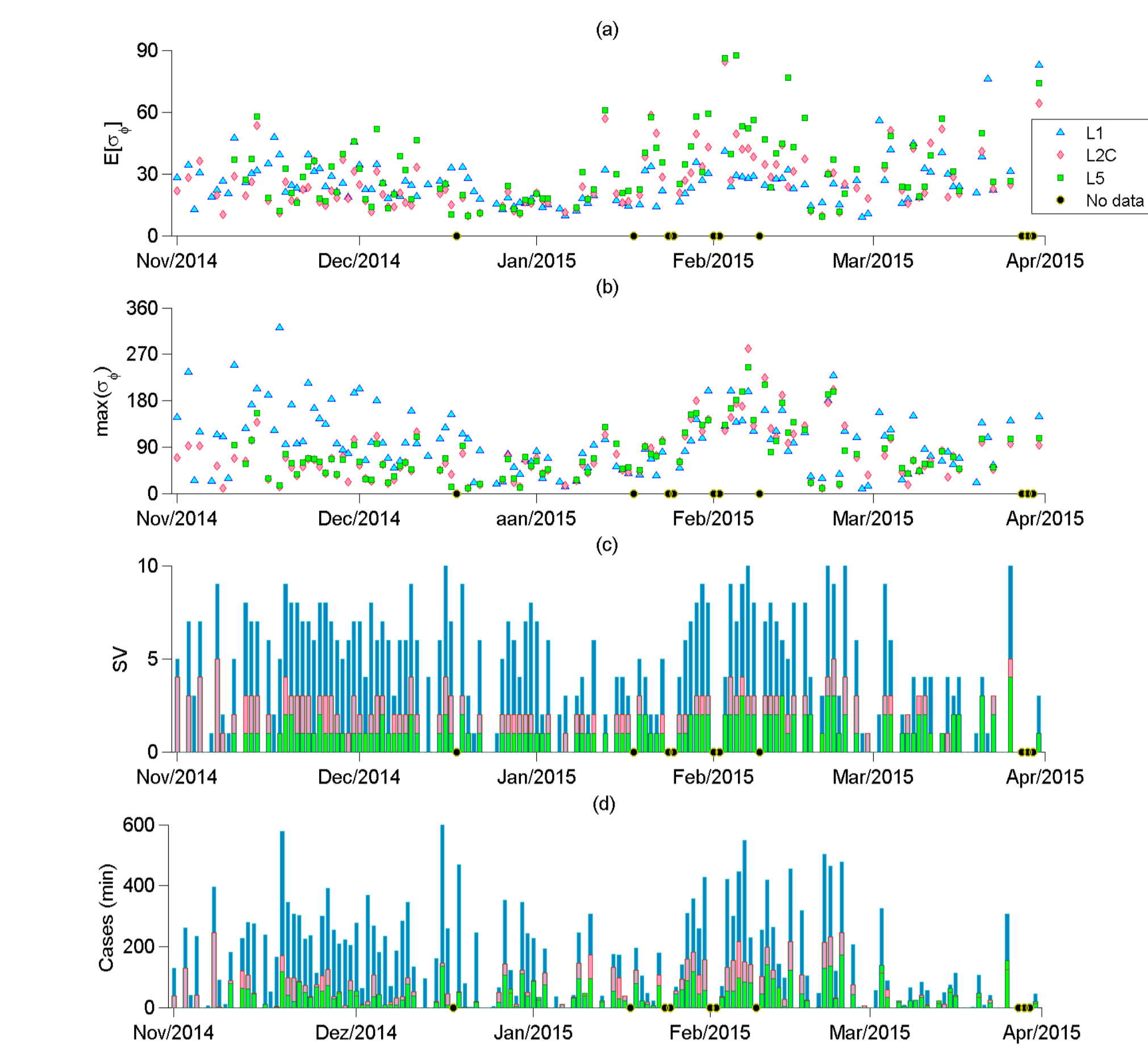


**Figure 2** – (a) Daily average value for  $\sigma_\phi$  from November 1, 2014 to March 31, 2015 (b) Daily maximum value registered for  $\sigma_\phi$  (c) Total number of satellites affected every night (d) Total of cases recorded each night for  $\sigma_\phi > 8.6^\circ$ . Only occurrences with five minutes or more of transmissions with  $\sigma_\phi > 8.6^\circ$  were considered in the above plots.

## 3) $\sigma_\phi$ Local Time Distribution:

For different intensity ranges, more than 75% of the cases corresponded to  $\sigma_\phi < 30^\circ$ . Additionally, during the absolute peak intervals for moderate phase scintillation, 76.4 %, 86.8 %, and 86.5 % of the cases are such that  $\sigma_\phi < 30^\circ$  for the L1, L2C, and L5 frequencies, respectively. Scintillation with  $\sigma_\phi < 30^\circ$  starts around 1930 LT (Figure 3), to reach its peak occurrence from 2200 LT to 2330 LT at the L1 frequency. However, the peak occurrence shifts to later hours (from 2300 LT to 2330LT) at the lower frequencies L2C and L5. The stronger scintillation ( $\sigma_\phi > 30^\circ$ ) started around 2000 LT, the occurrence maximizing between 2100 LT and 2130 LT, one hour sooner than the peak in weak scintillation. During the peak occurrence, the percentage of the strong cases is 34.8 % at L1 and this percentage increased with the decrease in frequency, being 38.2 % at L2C and 55.8 % at L5.

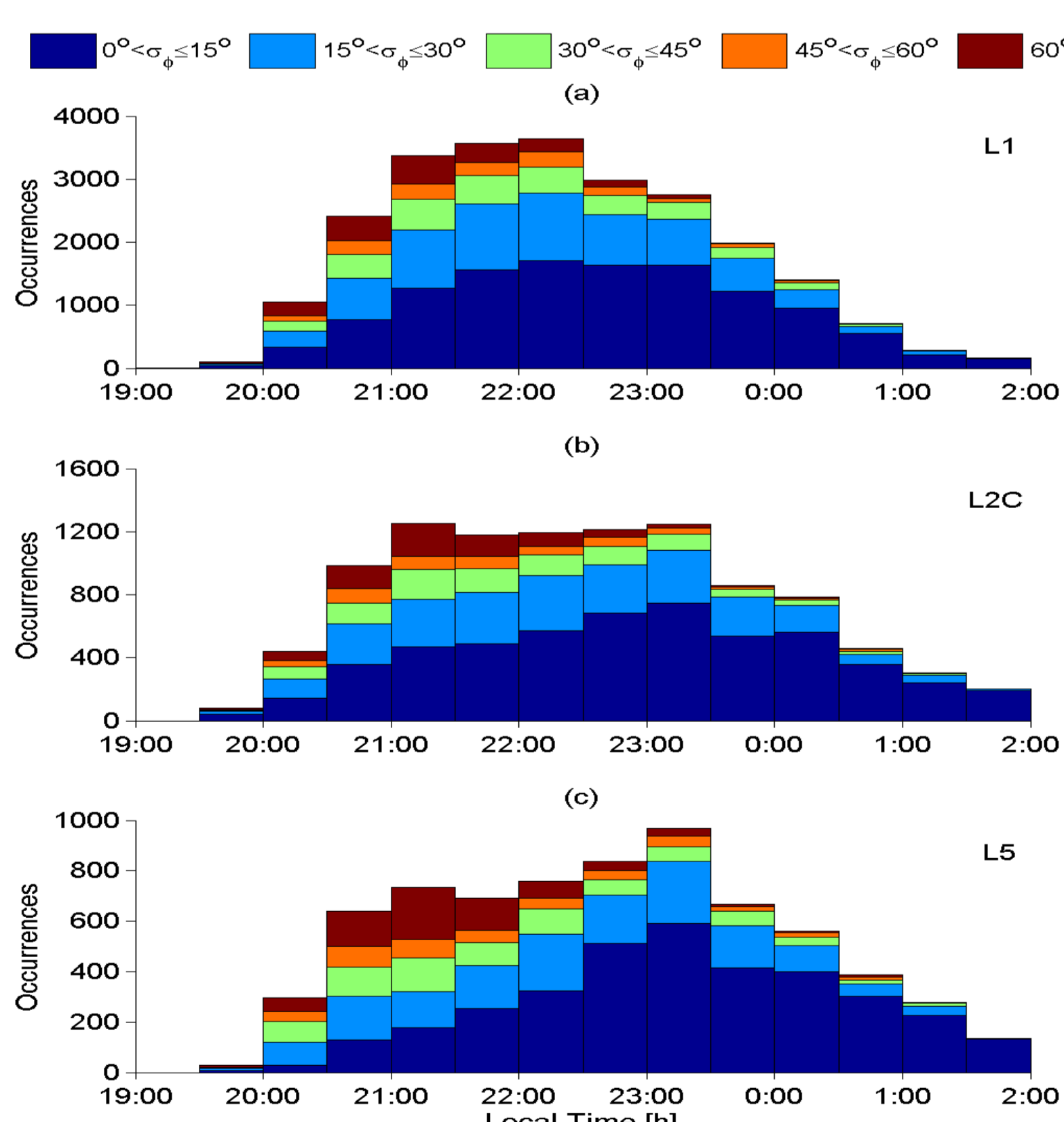


**Figure 3** – Histograms of the  $\sigma_\phi$  index as functions of local time intervals, for different levels of phase scintillation activity and the three frequencies. Panels 3(a), 3(b), and 3(c) correspond to the L1, L2C, and L5 frequencies, respectively.

## 4) $\sigma_\phi$ Spatial Distribution:

The azimuth and elevation distributions of phase scintillation, as seen from the receiver location, were examined for different ranges of  $\sigma_\phi$  values at the three frequencies. It was noted that there is a dominance of  $\sigma_\phi$  for azimuths around 345° at all levels of phase scintillation. This observation strongly suggests an association with plasma bubbles elongated in the magnetic meridian plane through the receiver location (at a westward magnetic declination angle of 21.4°). It also points to phase scintillation resulting from refractive effects integrated along signal paths running nearly along field-aligned EPBs. Fewer cases of phase scintillation were observed from the northeastern direction, more dominantly at the lower frequencies. More recent cases of  $\sigma_\phi$  were observed at elevation angles greater than 36°, which may be indicative of the vertical growth rate for the bubble to reach appropriate apex heights over the equator that can contribute towards EPB-aligned line-of-sights from the receiver. It was also noted that intense phase scintillation was observable at higher elevation angle (around 60°) at the lower frequency (L5).

A most noteworthy aspect is that no significant scintillation cases could be observed from the southern quadrants (180° - 270°) of the receiver, which is an indication that, during the observational period (November 2014-March 2015), which is close to the recent solar maximum, the EPBs did not rise up to more than about 900 km over the equator, the apex height of the magnetic field line mapping to the F region over São José dos Campos.

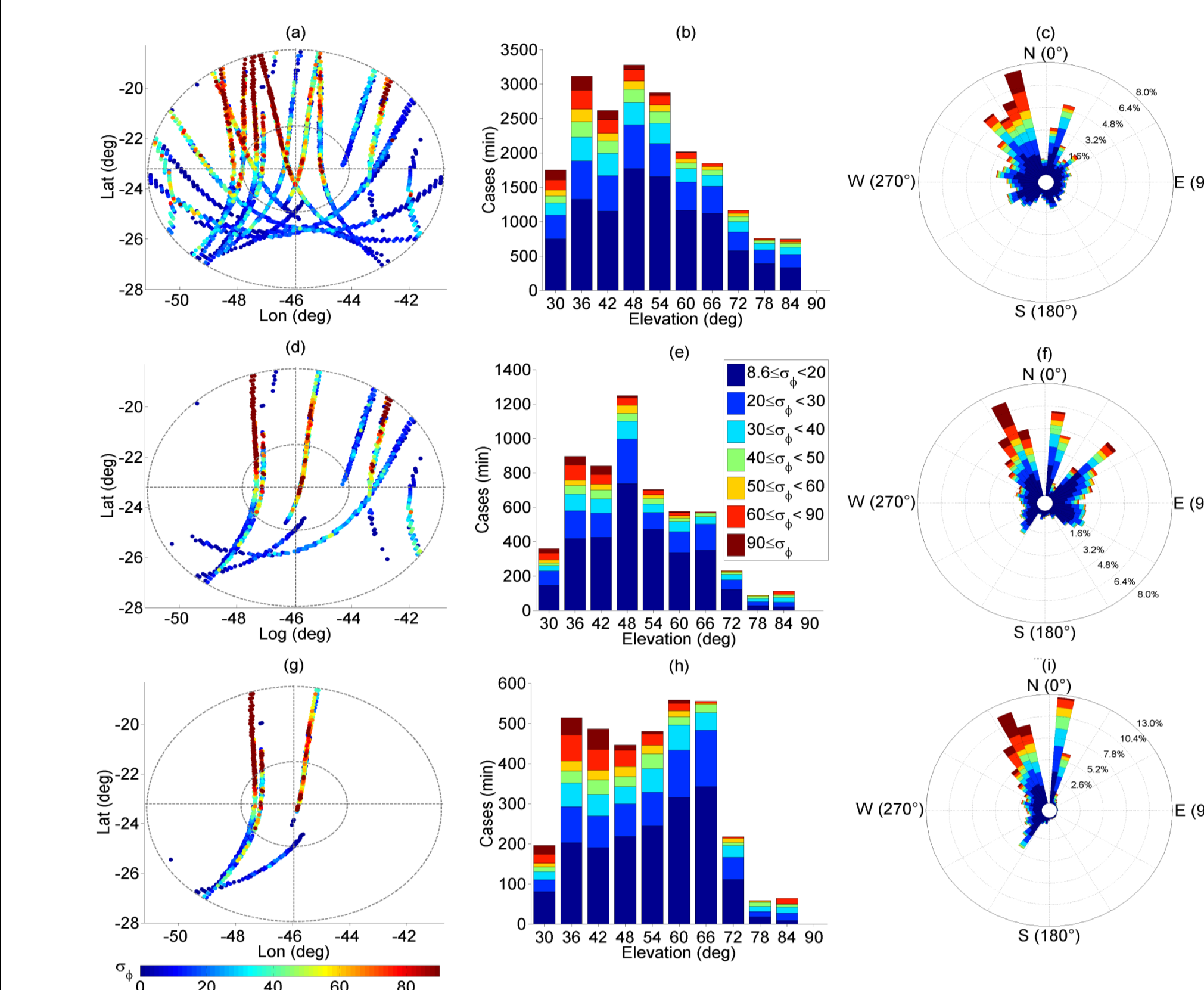


**Figure 4** – The spatial distribution of phase scintillation events. The top, central and bottom rows of panels represent results for L1, L2C, and L5 measurements. The left-hand side panels (a), (d), and (g) show the IPP distribution of phase scintillation. The central panels (b), (e), and (h) show the statistical distribution of  $\sigma_\phi$  as a function of elevation. The right-hand side panels (c), (f), and (i) show statistical distribution of  $\sigma_\phi$  as function of azimuth.

## 5) S4 and $\sigma_\phi$ comparison:

Each of the three frequencies showed a well-defined relationship between them. However, there are non-negligible numbers of simultaneous cases of high values of S4 and low values of  $\sigma_\phi$ , and vice-versa. A somewhat linear relationship between S4 and  $\sigma_\phi$  values averaged over discrete intervals was observed for  $\sigma_\phi < 70^\circ$ . The corresponding average S4 values are found to be slightly larger at the lower frequency. Also, S4 values tended to saturate for larger  $\sigma_\phi$  values, exceeding around 80°. This suggests that, for severe events, phase measurement can provide a better evaluation of scintillation variability than it is possible from amplitude measurement. It was also observed that the number of phase scintillation events decreases with increasing  $\sigma_\phi$  values. Such decrease occurs at a faster rate for smaller S4 values and at a slower rate for larger S4 values. At the lower frequency (L5), both rates are slightly slower than those for the higher frequency (L1). Further, it was noticed that, for small S4 values, the number of  $\sigma_\phi$  cases decreases with  $\sigma_\phi$  at a rate that is significantly faster than the corresponding rate of S4 for small  $\sigma_\phi$  values. This observation seems to indicate that the combination of intense amplitude scintillation and weak phase scintillation is more common than the opposite.

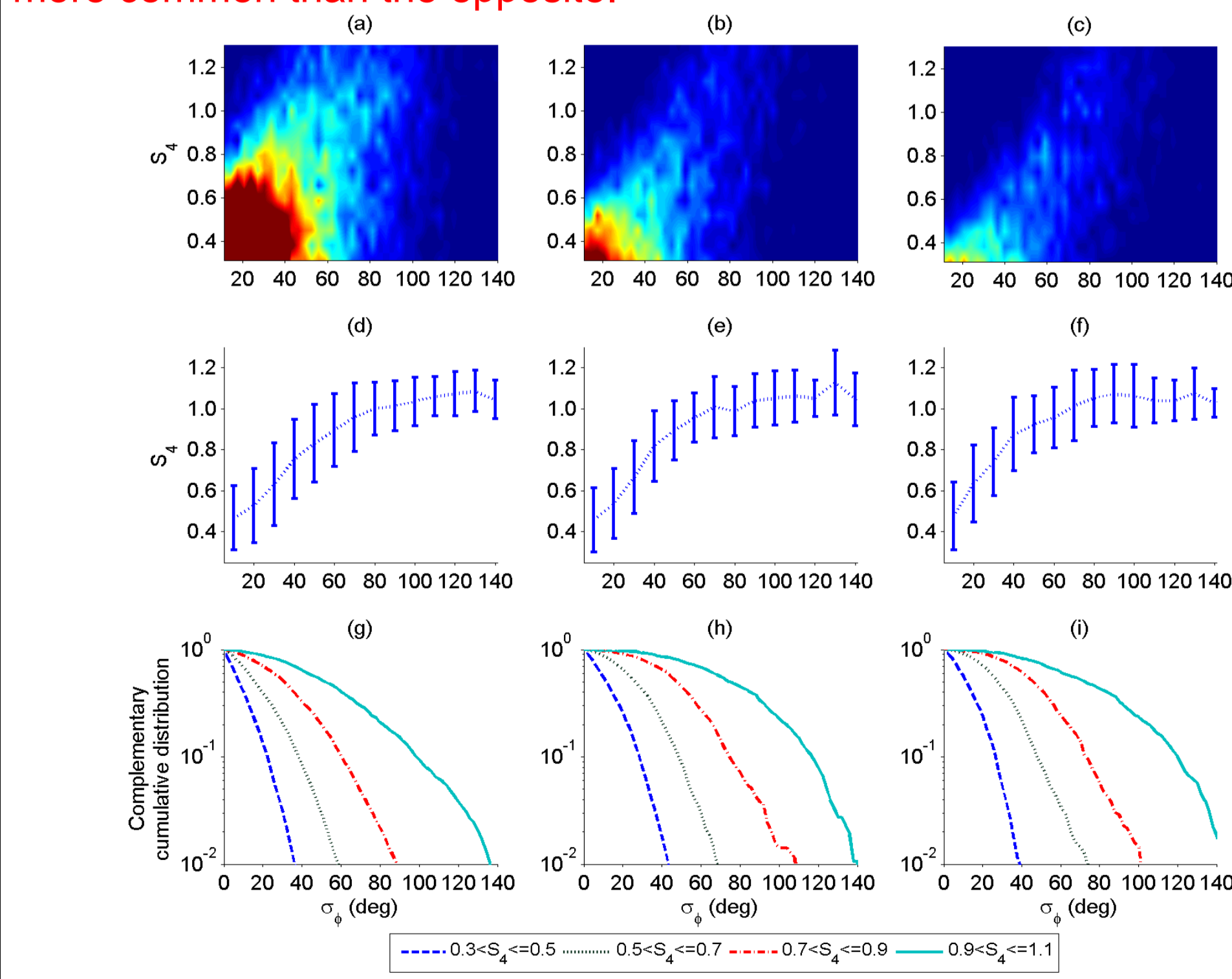


**Figure 5** – Panels (a), (b), and (c) show occurrence map for combinations of S4 and  $\sigma_\phi$  values, using the upper-right color scale (number of cases). Panels (d), (e), and (f) show average value for S4 as function of  $\sigma_\phi$ , as well as the associated standard-deviation bars. Panels (g), (h), and (i) display complementary cumulative distribution of  $\sigma_\phi$  for different S4 ranges. From left to right, the columns refer to the L1, L2C, and L5 signals, respectively.

## 6) Amplitude and Phase Correlation:

A detailed study showed that, although most cases of  $\sigma_\phi$  and S4 are highly correlated, there is a substantial number of examples of poor to moderate correlations. The total percentages of weak, moderate, and strong correlation cases for the L1 frequency (Figure 6) are 14 %, 28 %, and 58 %, respectively. It was also found that, in the lower ranges of values of  $\sigma_\phi$  ( $< 30^\circ$ ) and S4 ( $< 0.7$ ), the percentages of cases with weak, moderate, and strong correlation are nearly the same (35.16 %, 30.07 % and 34.07 %, respectively). On the other hand, for higher values of  $\sigma_\phi$  ( $> 30^\circ$ ) and S4 ( $> 0.7$ ), the corresponding percentage of the cases are 0.00 %, 15.85 %, and 84.15 % respectively, indicating the dominance of cases of strong correlation for more intense scintillation. The circumstances that control the degree of correlation are not clearly identified. However, it can be noticed in the examples of Figures 6(d) to 6(i) that the highest degrees of correlation are generally present in the earlier stage of scintillation events or during the increasing stage of strong scintillation episodes. Correlation seems to be poorer during the decreasing stages of the scintillation activity. There are exceptions to this general tendency that need to be investigated further.

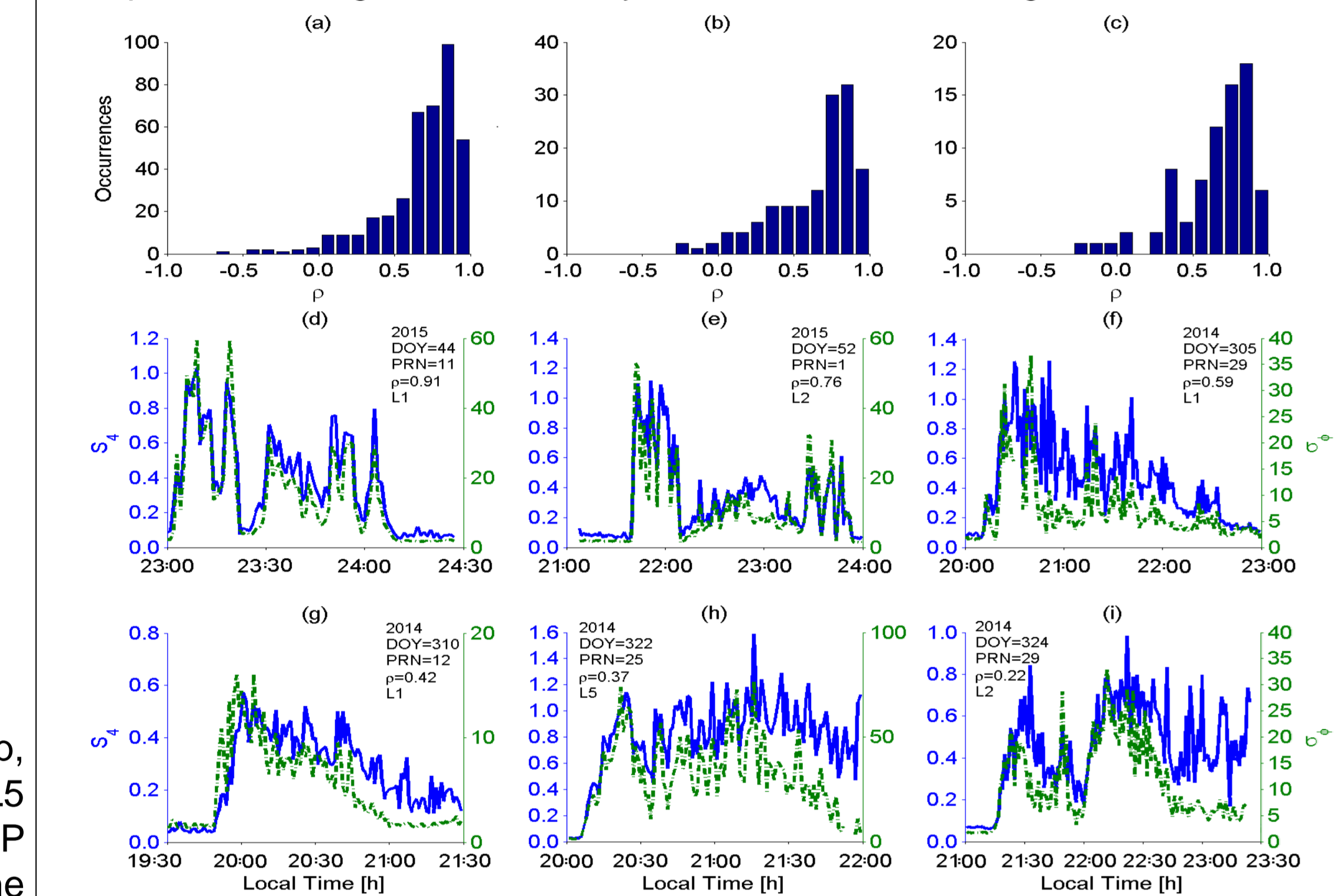


**Figure 6** – Panels (a), (b), and (c) show the distribution of the correlation coefficient  $\rho$  for the L1, L2C, and L5 signals, respectively. Panels (d), (e), (f), (g), (h), (i) display examples of S4 and  $\sigma_\phi$  relation for different values of  $\rho$ .

## 7) Frequency Dependency of Scintillation:

A more direct analysis on the frequency dependence of  $\sigma_\phi$  and S4 was carried out (Figure 7) with the objective of verifying the validity of theoretically-expected ratios of the scintillation indices at the different frequencies. This investigation was carried out to support evaluations of the severity of scintillation at the new lower frequency L5 (intended for aeronautical applications) based on the values at the more widely used L1 frequency. The result showed that the ratios of phase scintillation indices were in excellent agreement with their expected values (that is, the corresponding frequency ratios) until a transition value of  $\sigma_\phi = 100^\circ$  is reached. In the case of amplitude scintillation (for which the expected ratio was the frequency ratio raised to the power 3/2) the transition occurred at S4 = 0.6. Above these transition values, the ratios decrease with increase in scintillation intensity. In other words, the relationships tended to saturate with further increase in the scintillation intensity at L1. However, the scintillation ratio between the two closer frequencies L2C and L5 maintained its expected value at all levels of scintillation intensity.

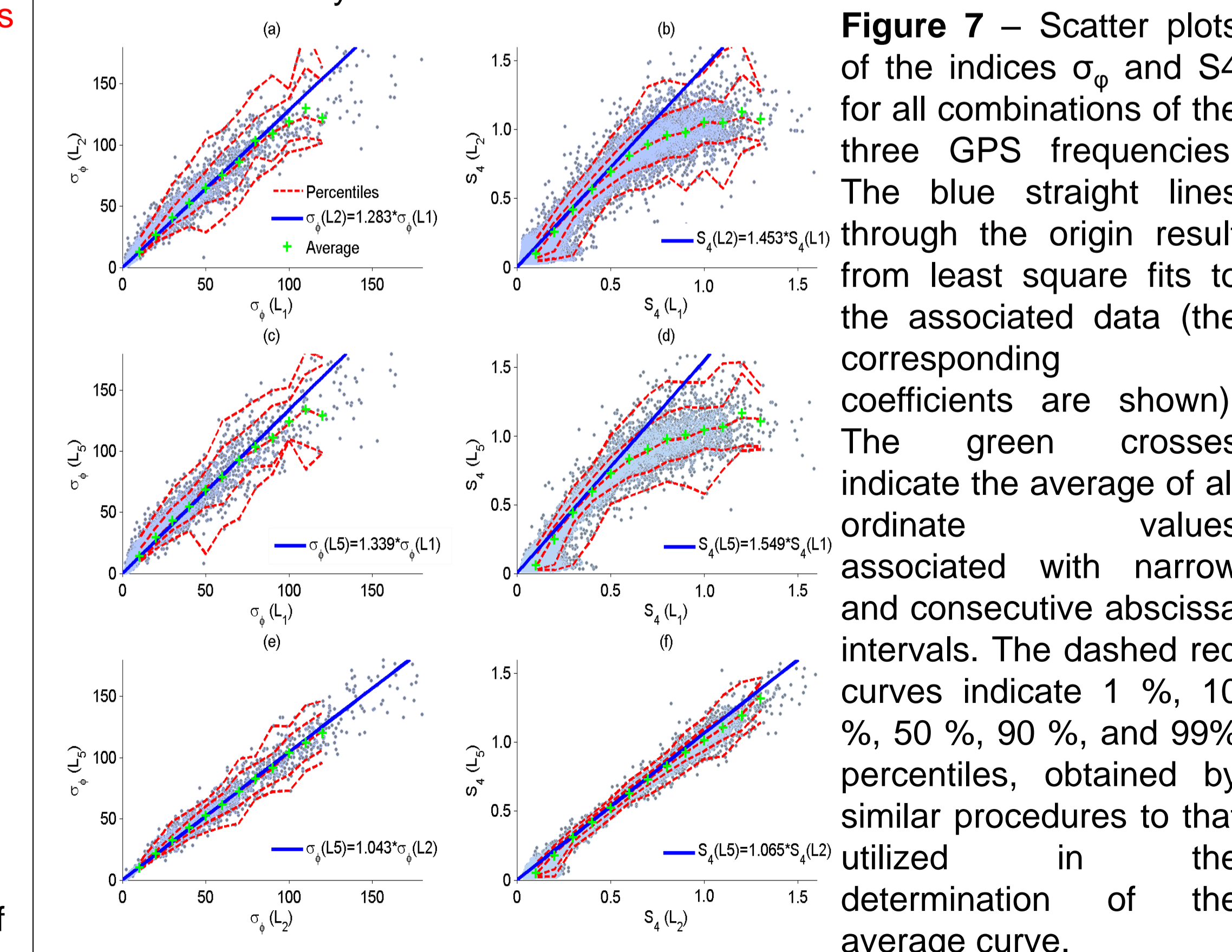


**Figure 7** – Scatter plots of the indices  $\sigma_\phi$  and S4 for all combinations of the three GPS frequencies. The blue straight lines through the origin result from least square fits to the associated data (the corresponding coefficients are shown). The green crosses indicate the average of all ordinate values associated with narrow and consecutive abscissa intervals. The dashed red curves indicate 1 %, 10 %, 50 %, 90 %, and 99% percentiles, obtained by similar procedures to that utilized in the determination of the average curve.

**Reference:** Moraes, A.O, E.Costa, F.S. Rodrigues, M.A.Abdou, E.R. de Paula, K. Oliveira, W.J. Perrella, The variability of Low-Latitude Ionospheric Amplitude and Phase Scintillation Detected by a Triple Frequency GPS Receiver, Submitted to Radio Science, 2015.